Eigenvalue density oscillations in separable microwave resonators

Olaf Frank* and Bruno Eckhardt
Fachbereich Physik und Institut für Chemie und Biologie des Meeres, Carl von Ossietzky Universität, Postfach 25 03, D-26111 Oldenburg, Germany
(Received 28 July 1995)

We study periodic orbit induced oscillations in the density of states for the electromagnetic eigenvalue problem in separable three-dimensional resonator geometries. The periodic orbit theory of Berry and Tabor [J. Phys. A **10**, 371 (1977)] is adapted to the eigenvalue problem for the transverse electric and magnetic modes, respectively. Discrete symmetries give rise to next to leading order corrections, as is demonstrated in particular for cylinders with square and triangular cross sections. In particular, orbits with an odd number of reflections that do not contribute in leading order according to results of Balian and Duplantier [Ann. Phys. (N.Y.) **104**, 300 (1977)] are shown to contribute in next to leading order.

PACS number(s): 05.45.+b

I. INTRODUCTION

Measurements on flat microwave resonators have recently been used to investigate properties of the Helmholtz equation in the short wavelength limit [1–3]. These resonators are of cylindrical shape and flat in the sense that for several hundred of the lowest lying states the electromagnetic field is in a transverse magnetic mode with an **E** component along the axis of the cylinder. Then the eigenvalue problem reduces to that for a two-dimensional (2D) Helmholtz equation for a scalar field, which vanishes on the boundaries. It is this reduction in dimensionality that allows one to transfer all results from standard short wavelength or "semiclassical" theory [4] to the electromagnetic eigenvalue problem in a flat cavity. It is the purpose of this paper to investigate some of the changes that occur when the cavity is not flat, i.e., when excitations in all three directions mix.

The electromagnetic eigenvalue problem is distinguished from the corresponding scalar problem by the presence of the polarizations of the field. Nevertheless, the semiclassical expansion for the density of states turns out to be very similar to that for the scalar problem [5]. It splits into a mean density of states, which now doubles because of the two possible polarizations and an oscillatory contribution from orbits that close after a certain number of reflections off the walls. The analysis of Balian and Duplantier [5] shows that the contributions from orbits with an odd number of reflections are suppressed in leading order stationary phase approximation compared to the amplitudes of the orbits for scalar fields. The amplitude for an orbit with an even number of reflections is $2\cos\psi$ times that for the scalar problem if the polarization is rotated by an angle ψ along the periodic orbit. This may be understood by following a plane wave around the orbit. At every reflection, the polarizations change by a reflection in a plane perpendicular to the direction of propagation. After an odd number of reflections, there remains a reflection in that plane so that the trace over the polarizations vanishes. After an even number of reflections the total change is a rotation with trace $2\cos\psi$.

Below we will focus on empty cylindrical cavities with perfectly conducting walls [6,7]. Then the electromagnetic eigenvalue problem may be separated into two scalar ones for the so-called transverse electric and transverse magnetic modes. If the axis of the cylinder is parallel to the z axis, one can write for the TM modes

$$\mathbf{B}(x,y,z,t) = \mathrm{curl}\, f_M(x,y,z)\mathbf{e}_z e^{i\omega t} \tag{1}$$

and

$$\mathbf{E}(x,y,z,t) = \frac{i}{\omega}\mathrm{curl}\,\mathrm{curl}\, f_M(x,y,z)\mathbf{e}_z e^{i\omega t}\,, \tag{2}$$

where f_M has to satisfy the 3D Helmholtz equation

$$\left(\frac{\partial^2}{\partial x^2}+\frac{\partial^2}{\partial y^2}+\frac{\partial^2}{\partial z^2}+k^2\right) f_M = 0\,. \tag{3}$$

$k=\omega/c$, with c the speed of light, is the wave number. Because of the z independence of the cross section and the boundary conditions that the tangential component of **E** at top and bottom of the cylinder has to vanish, one can split off the z dependence (parametrized by an integer p) and write

$$f_M(x,y,z) = \psi_M(x,y)\cos(p\pi z/H) \tag{4}$$

for a cylinder that extends between $0 \le z \le H$. Then ψ_M satisfies the 2D Helmholtz equation

$$\left(\frac{\partial^2}{\partial x^2}+\frac{\partial^2}{\partial y^2}+k_M^2\right)\psi_M = 0\,, \tag{5}$$

*Present address: Fakultät für Physik, Albert-Ludwigs-Universität, Hermann-Herder-Str.3, D-79104 Freiburg, Germany.

with $k_M^2 = k^2 - \pi^2 p^2/H^2$ and with the boundary condition that ψ_M vanishes on the sides. Thus f_M satisfies Neumann boundary conditions at the top and bottom and Dirichlet boundary conditions at the sides.

For the TE modes one proceeds in an analogous fashion, starting from

$$\mathbf{E}(x,y,z,t) = \mathrm{curl}\, f_E(x,y,z)\mathbf{e}_z e^{i\omega t} \tag{6}$$

and

$$\mathbf{B}(x,y,z,t) = -\frac{i}{\omega}\mathrm{curl}\,\mathrm{curl}\, f_E(x,y,z)\mathbf{e}_z e^{i\omega t}\ , \tag{7}$$

where f_E satisfies the same 3D Helmholtz equation as f_M. However, the boundary conditions change: f_E now satisfies Neumann boundary conditions at the sides and Dirichlet boundary conditions at top and bottom. Thus f_E factorizes into

$$f_E(x,y,z) = \psi_E(x,y)\sin(p\pi z/H), \tag{8}$$

where ψ_E is a solution to the 2D Helmholtz equation with Neumann boundary conditions at the sides. For further details, see [6,7].

Because of this separability one can reduce the electromagnetic eigenvalue problem to two scalar ones where the semiclassical trace formula can be applied. The total spectrum, including degeneracies, is then given by the superposition of the two scalar ones. This suggests another argument for the suppression of orbits with an odd number of reflections. Let an orbit close after r reflections off the top and bottom and s reflections off the sides. Note that for a periodic orbit in a cylindrical cavity the number of reflections off the top and bottom is always even, so that the total number of reflections is an even number plus the number of reflections off the sides of the cavity. At the sides with Dirichlet boundary conditions, the phase loss is π for each reflection, whereas at the sides with Neumann boundary conditions there is no phase loss. Thus, the total phase change for an orbit contributing to the spectra of the TM and TE subspaces is $-s\pi \bmod 2\pi$ and 0π, respectively. In a superposition of the two spectra, the contributions from orbits with an odd number of reflections will have a phase difference of $-\pi$ between the two subspaces and will thus cancel out. For an even number of reflections a factor of 2 is obtained. As there are no phase rotations along any periodic orbit for cylindrical cavities, the result is in perfect agreement with the more general theory of Balian and Duplantier [5].

The easiest way to check this theory is by a suitable Fourier transform of the density of states that reveals the amplitudes and phases of the periodic orbit contributions. Specifically, the semiclassical trace formula for the density of states in wave number of N-dimensional integrable billiards (electromagnetic or scalar) is of the form (Berry and Tabor [8])

$$\rho(k) = \rho_0(k) + 4\,\mathrm{Re}\sum_p k^{(D-1)/2} A_p e^{ikL_p}, \tag{9}$$

where L_p is the length and D the degeneracy of the periodic orbit. Degeneracy here means the number of directions in which the position of the orbit in the cavity can be altered continuously without changing its shape on the energy shell. $\rho_0(k)$ denotes the smooth Weyl approximation (which is of no concern here) and the amplitudes A_p are determined by the geometry of constant energy surfaces in action space. The dominant scaling of the amplitudes with energy or wave number has been taken out by the factor $k^{(D-1)/2}$; the detailed form of the k dependence of the A_p, as well as subdominant k dependencies will be discussed below.

If $w(k)$ denotes a normalized window function in wave number space and

$$\tilde{w}(l) = \frac{1}{2\pi}\int_{-\infty}^{+\infty} dk\, w(k)\, e^{ikl} \tag{10}$$

its Fourier transform in length space (length being canonically conjugate to wave number), then

$$\begin{aligned}\frac{1}{2\pi}\int_{-\infty}^{+\infty} dk\, \frac{1}{2}\rho(k)k^{(1-D)/2}w(k)\, e^{ikl} \\ = \frac{1}{2\pi}\int_{-\infty}^{+\infty} dk\, \rho_0(k)k^{(1-D)/2}w(k)\, e^{ikl} \\ + \sum_p 2A_p\delta(l-L_p)\otimes\tilde{w}(l)\,,\end{aligned} \tag{11}$$

where $\otimes$ denotes the convolution product, reveals the amplitudes of the orbits. This is because the factor $k^{(1-D)/2}$ eliminates the k dependence of the amplitude factors and the amplitude of the periodic orbit is just a real or complex number. The term, involving $\rho_0(k)$, gives a contribution of high amplitude at very small lengths according to the Fourier transform of a monotonically growing function in k space.

In Sec. II we will present Fourier transforms of the wave number spectra as obtained for cylindrical cavities with circular, square, and triangular cross sections. The shown spectra give the absolute values of the Fourier transforms, except for Fig. 2, where the cosine transform is shown. To calculate the numerical spectra we used a Gaussian distribution centered at the middle a of the considered k range, and a width $\sigma = 20$,

$$w(k) = \frac{1}{\sqrt{2\pi}\sigma}\exp[-(k-a)^2/2\sigma^2]\,. \tag{12}$$

The peak height is normalized to one for the Fourier transformed window function.

The Fourier transforms reveal next to leading order corrections, which can be understood as corrections to the density of states due to orbits on the boundary of the billard or due to other symmetry related effects. The formal theory is worked out in Sec. III. We conclude with a short summary in Sec. IV.

II. EIGENVALUES IN CYLINDRICAL CAVITIES

A. Circular cross section

The Helmholtz equation in a circular domain separates in polar coordinates [6]. The solutions are thus propor-

tional to

$$\psi(x,y) \sim J_{|\nu|}(kr)e^{i\nu\phi}, \tag{13}$$

where r, ϕ are polar radius and angle, respectively. To preserve periodicity in the azimuthal direction, ν has to be an integer, $\nu = 0, \pm 1, \pm 2, \ldots$. For Dirichlet boundary conditions, the appropriate wave numbers $k^{(D)}_{\nu,m}$ are determined by the zeroes of the above functions at the boundary $r = R$,

$$J_\nu(k^{(D)}_{\nu,m}R) = 0\,. \tag{14}$$

Similarly, for Neumann boundary conditions, the appropriate wave numbers $k^{(N)}_{\nu,m}$ are determined by the zeroes of the radial derivatives of the above functions at the boundary $r = R$,

$$J'_\nu(k^{(N)}_{\nu,m}R) = 0\,. \tag{15}$$

Each eigenvalue for $\nu \neq 0$ is doubly degenerate because of the two choices ν and $-\nu$. Thus the eigenvalues of the electromagnetic cylindrical resonator with circular cross section of radius R and height H are given by

$$k_{l,\nu,m} = \sqrt{\left(k^{(D)}_{\nu,m}\right)^2 + (\pi l/H)^2}\,, \tag{16}$$

$l = 0, 1, 2, 3 \ldots$, doubly degenerate for $\nu \neq 0$ and

$$k_{l,\nu,m} = \sqrt{\left(k^{(N)}_{\nu,m}\right)^2 + (\pi l/H)^2}\,, \tag{17}$$

$l = 1, 2, 3, \ldots$, also doubly degenerate for $\nu \neq 0$.

The Fourier transform of all eigenvalues up to $k = 200$ for a resonator with radius $R = 1$ and height $H = \pi$ (a total of 1 320 508 eigenvalues for the scalar field with Dirichlet BC and 2 937 855 for the electromagnetic field) with the window (1) is shown in Fig. 1. One notes a series of isolated peaks that can be assigned to periodic orbits that have the topology indicated by the numbers above the peaks. The first number gives the bounces off the walls, the second the number of revolutions about the center of the disc, and the third the number of reflections off the top and bottom. Rather noticeable is the poor resolution near lengths $L_{n,p} = \sqrt{(2\pi n)^2 + (2\pi p)^2}$ for integer p, n, which correspond to orbits that go around the cylinder once or several times, with or without translation along the symmetry axis. These orbits are an example of whispering gallery modes and are accumulation points of an infinite family of orbits with an increasing number of reflections off the outer circle. They occur also in the stadium billiard (see [3]) and in the sphere (see [9]).

More important in the present context are the noticeable, but small amplitudes that come with orbits with an odd number of reflections off the walls. In agreement with the theory of Balian and Duplantier [5] their amplitude is smaller and of lower order in k for the electromagnetic field than for the scalar field (i.e., it decays further if larger intervals in k are Fourier transformed). Nevertheless, by the argument about the phases given in the introduction one might have expected the amplitudes of these orbits to disappear completely. To analyze this behavior further we show in Fig. 2 the cosine transforms of the spectra of the 2D Helmholtz equation with Dirichlet and Neumann boundary conditions, respectively. This clearly shows that within numerical accuracy, all orbits

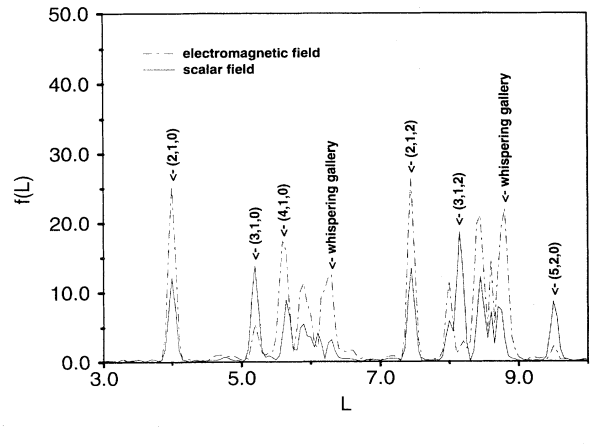

FIG. 1. Fourier transform of the electromagnetic eigenvalue density for a cylindrical cavity of circular cross section (height π, radius 1, including the lowest 1 320 508 eigenvalues for the scalar field and 2 937 855 eigenvalues for the electromagnetic field of wave number $k < 200$). The labels (m, n, p) above the peaks give the numbers m of radial oscillations, n of rotations around the center, and p of vertical collisions. The total number of collisions is thus $m + p$.

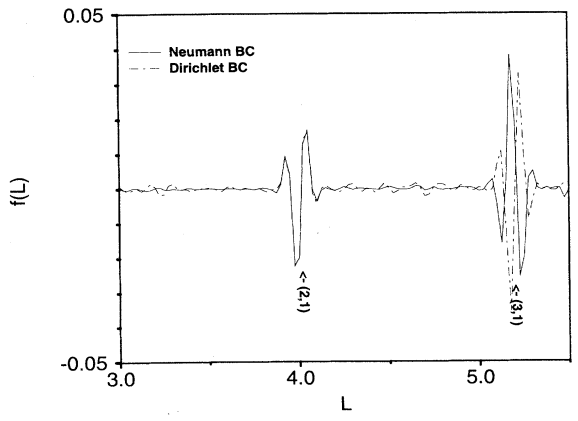

FIG. 2. Cosine transforms for the scalar eigenvalue problem in a circle of radius 1 with Dirichlet and Neumann boundary conditions. For the orbits with an odd number of reflections the amplitudes for Neumann and Dirichlet boundary conditions have different signs. All 36 647 eigenvalues for Neumann and 39 940 eigenvalues for Dirichlet boundary conditions with $k < 400$ are included.

carry the same amplitudes, but alternating phases. In a superposition of the two eigenvalue sets the contributions from orbits with an odd number of bounces thus cancel. The remaining amplitude seen in Fig. 1 is related to the top and bottom boundary conditions, which are similar to the ones at the sides of a square, to which we turn now.

B. Square cross section

In a cylindrical cavity with square cross section the wave equation separates in the three directions. The calculation of eigenvalues is straightforward and yields

$$k_{m,n,p} = \sqrt{\left(\frac{m\pi}{d}\right)^2 + \left(\frac{n\pi}{d}\right)^2 + \left(\frac{p\pi}{H}\right)^2}, \qquad (18)$$

where d is the side length of the square and H the height in the z-direction with $0 \le z \le H$. For TM modes one has $n, m = 1, 2, \ldots$ and $p = 0, 1, \ldots$ and for TE modes $n, m = 0, 1, \ldots$ and $p = 1, 2, \ldots$. As there are no orbits with an odd number of bounces off the walls in the square, we expect no cancellations.

However, there is a slight difference between the amplitudes for TE and TM modes (not shown). To investigate this difference further we again turn to a lower dimensional example, the 2D square billard. Taking the sides of the square to be π, the eigenvalues are $n^2 + m^2$ with $n, m = 0, 1, 2, \ldots$ for Neumann boundary conditions and with $n, m = 1, 2, \ldots$ for Dirichlet boundary conditions. The amplitudes of some of the periodic orbits are found to be different for Dirichlet and Neumann boundary conditions as shown in Fig. 3. This effect, which is also

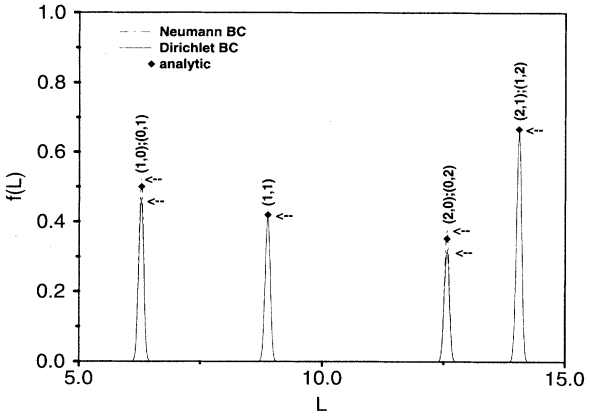

FIG. 3. Fourier transforms for the scalar eigenvalue problem in a square of sidelength π with 70 370 eigenvalues for Dirichlet and 70 969 eigenvalues for Neumann boundary conditions with $k < 300$. The k dependence of the amplitudes is taken out. There is no difference in phase (since the number of reflections of all orbits is even), but a slight difference in amplitude, indicated by the arrows. This difference is of lower order in wave number since it varies if longer sequences of eigenvalues are Fourier transformed, but it stabilizes if Fourier transforms with $D = 1$ in Eq. (11) are taken.

responsible for the nonperfect cancellations in the case of the 3D circular cylinder, will be explained by corrections due to a symmetry decomposition in the following sections.

C. Triangular cross section

We take a triangle with corners at $(0, h)$ and $(\pm h\sqrt{3}/2, -h/2)$. The solutions of Eq. (5) are then given by [7]

$$\psi_D(x,y) \sim \sin\left[\frac{l\pi}{h}y\right] f\left[\frac{\pi}{\sqrt{3}h}(m-n)x\right] + \sin\left[\frac{m\pi}{h}y\right] f\left[\frac{\pi}{\sqrt{3}h}(n-l)x\right] + \sin\left[\frac{n\pi}{h}y\right] f\left[\frac{\pi}{\sqrt{3}h}(l-m)x\right] \qquad (19)$$

for Dirichlet boundary conditions and by

$$\psi_N(x,y) \sim \cos\left[\frac{l\pi}{h}y\right] f\left[\frac{\pi}{\sqrt{3}h}(m-n)x\right] + \cos\left[\frac{m\pi}{h}y\right] f\left[\frac{\pi}{\sqrt{3}h}(n-l)x\right] + \cos\left[\frac{n\pi}{h}y\right] f\left[\frac{\pi}{\sqrt{3}h}(l-m)x\right] \qquad (20)$$

for Neumann boundary conditions. Here $h = \sqrt{3}L/2$ is the height of the equilateral triangle of side length L and $f(x) = \sin(x)$ or $\cos(x)$; the two choices correspond to functions symmetric or antisymetric around the symmetry line $x = 0$. The integers l, m, n are restricted by $l + m + n = 0$ and $l \le m \le n$. States with $n = m$ or $m = l$ are nondegenerate, and all others are doubly degenerate. In the case of Dirichlet boundary conditions l, m, n have to be nonzero since otherwise the wave functions vanish identically. These integers are related to the wave number by

$$k^2_{l,m,n} = \frac{2\pi^2}{3h^2}(l^2 + m^2 + n^2). \qquad (21)$$

The third dimension is added as in the preceding cases.

In the equilateral triangle there is a periodic orbit with an odd number of reflections off the walls. This is the orbit that connects the midpoints of the three sides of the triangle and any odd traversal of this orbit (see Fig. 4). The contribution of this orbit is in lower order in k since it has one continuous degeneracy less than the dominant ones [cf. Eq. (9)], but unlike in the case of the cylinder with circular cross section the amplitude is the same in the electromagnetic and in the scalar case. This is shown in Fig. 5. Considering the two-dimensional equilateral triangle with different kinds of boundary conditions, we see that the orbit contributes for Dirichlet boundary conditions but does not for Neumann boundary conditions (Fig. 6). This shows that in next to leading order the cancellation of orbits with an odd number of reflections as predicted by the theory of Balian and Duplantier [5]

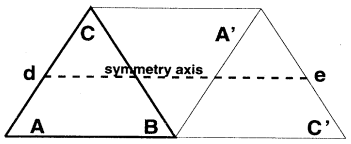

FIG. 4. Unfolding of the equilateral triangle and construction of the Möbius strip. Three copies of the triangle may be combined to a Möbius strip by identifying the points **A** and **A'**, as well as **C** and **C'**. The motion on the torus can then be visualized in the following way: One direction is along the Möbius strip, the other perpendicular to its axis with reflections on the upper and lower sides.

is violated. It can be related to symmetry properties of the two-dimensional triangle as discussed in Sec. III D.

III. BOUNDARY ORBITS

We will here study the effects of symmetries on the theory of Balian and Duplantier [5]. To establish the relation to the observations in Sec. II and to keep the formalism as low as possible, we will focus on the case of a 2D square with Dirichlet and Neumann boundary conditions. The symmetries are discussed in Sec. III A, followed by an outline of the theory of Berry and Tabor [8] in Sec. III B and the symmetry decomposition in Sec. III C. In the case of a triangular cross section one proceeds in a similar fashion. The main results are summarized in Sec. III D.

A. Symmetry effects in the 2D square

As Fig. 3 shows, the kind of deviations from the theory of Balian and Duplantier [5] observed in 3D electromagnetic billiards is already present for 2D squares with different boundary conditions. To leading order, the difference in boundary conditions only effects the phase of the amplitudes: for Dirichlet boundary conditions, there is a phase loss of π at each reflection, whereas there is no phase loss for Neumann boundary conditions. Thus, in a superposition of all eigenstates for both boundary conditions, the contributions of orbits with an even number of reflections double in amplitude and the ones for an odd number of reflections cancel. In the case of the square (and the rectangle, which we will not consider here, but which can be treated in the same way) there are no periodic orbits with an odd number of reflections. The observations (Fig. 3) confirm the phase effect but also reveal a difference in amplitude between transforms of spectra with Dirichlet and Neumann boundary conditions and on closer inspection also a deviation from the predictions of the semiclassical analysis of Berry and Tabor [8]. In the case of Neumann boundary conditions the amplitude is slightly too high, whereas it is too small for Dirichlet boundary conditions. The key to the explanation is that deviations occur for orbits parallel to the axes only. These families of orbits include the boundary of the billiard and require special care since they are invariant under some symmetries of the classical motion.

Symmetries affect the periodic orbit formalism in two ways [10]: if an orbit itself is symmetric, it may be subdivided into fundamental nonsymmetric segments, which contribute with amplitudes similar to the usual ones. More interesting in the present context are orbits which run within a symmetry plane of the system since their amplitudes often take on a different form than for other periodic orbits (for a worked out example, see [11]).

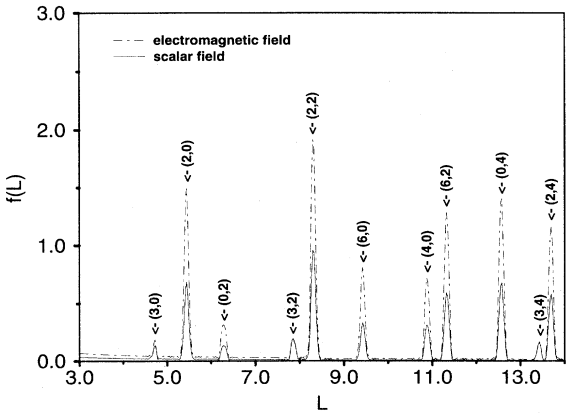

FIG. 5. Fourier transform of the electromagnetic eigenvalue density for a cylindrical cavity of triangular cross section (height π, side length of triangle π, including the lowest 922 293 eigenvalues of wave number $k < 100$ for the electromagnetic field and 451 788 eigenvalues of wave number $k < 100$ for the scalar field). The labels (m,n) above the peaks give the numbers of reflections in the x-y plane and z direction, respectively. The total number of collisions is $m+n$.

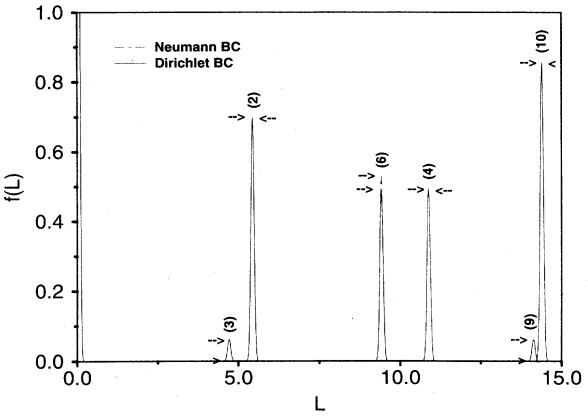

FIG. 6. Fourier transform for the scalar eigenvalue density for a two-dimensional cavity of triangular cross section with sidelength π for Neumann and Dirichlet boundary conditions on the sides. The numbers indicate the number of reflections on the boundary. The arrows indicate the difference in amplitude for Neumann and Dirichlet boundary conditions. Note that for three and nine reflections the amplitude for Neumann boundary conditions is zero. For Neumann boundary conditions we used the first 27 207 eigenvalues and for Dirichlet we used the first 26 908 eigenvalues.

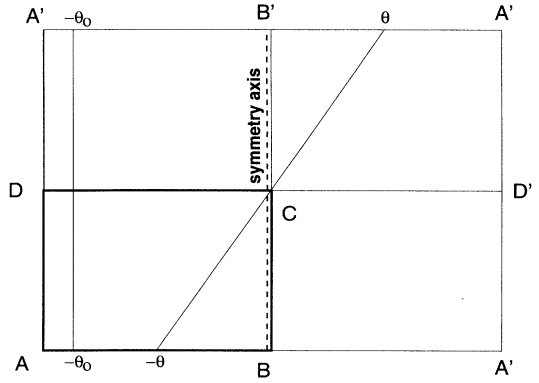

FIG. 7. Boundary orbits in a 2D square billiard. The square $ABCD$ is unfolded into $ABA'D'A'B'A'D$, which tiles the plane under translation. The symmetry axis considered is the line BCB'. The orbit $-\theta_0$, $-\theta_0$ is periodic for all $-\theta_0$, wheras the orbit $-\theta$, θ is periodic only if it coincides with the symmetry axis for $\theta = 0$.

To see the origin of the symmetry under which the boundaries of the square are invariant, consider the usual unfolding of the square onto the plane [12]. One starts by reflecting the square on its sides to form another square with four copies of the original one, as shown in Fig. 7. If the upper and the lower side as well as the left and the right side are identified, the dynamics is equivalent to the motion on a torus. Equivalently, the new square tiles the plane under translation and the eigenvalues and eigenfunctions are a subset of those of the torus with periodic boundary conditions. If the wave function satisfies Neumann boundary conditions on the sides of the original square, it is symmetric about the middle of the unfolded square. As we consider the motion on a torus the wave function is also symmetric about the outer walls of the unfolded square. In case of Dirichlet boundary conditions it is antisymmetric. The lines AD and BC are special in that they are invariant under reflection, which gives rise to modifications of the usual periodic orbit theory.

B. Theory of Berry and Tabor

The starting point of Berry and Tabor's considerations [8] is the energy dependent Greens function of the quantum mechanical system

$$G(\mathbf{r}_A, \mathbf{r}_B, E) = \int_0^\infty dt \exp[iEt/\hbar] K(\mathbf{r}_A, \mathbf{r}_B, t), \quad (22)$$

$$K(\mathbf{r}_A, \mathbf{r}_B, t) = \langle \mathbf{r}_B | \exp[-i\hat{H}t/\hbar] | \mathbf{r}_A \rangle. \quad (23)$$

The energy eigenvalue density $\rho(E)$ may be obtained from the trace of $G(\mathbf{r}_A, \mathbf{r}_B, E)$, leading to

$$\rho(E) = \mathrm{Re}\, \frac{1}{\pi\hbar} \int_0^\infty dt \exp[iEt/\hbar] \int d^N r K(\mathbf{r}, \mathbf{r}, t). \quad (24)$$

Berry and Mount [13] give a semiclassical approximation for the Greens function by means of the stationary phase approximation. The Greens function then depends only on the classical paths r of the system under consideration. Let $\mathbf{r}_A$ be the starting point, $\mathbf{r}_B$ the end point, W_r the action, and α_r the Maslov index, counting the number of caustics along the orbit. With N the number of degrees of freedom of the system and D_r the determinant of the Hessian of W_r with respect to the initial and final point of the path considered,

$$D_r(\mathbf{r}_A, \mathbf{r}_B, t) = \det\left(\frac{\partial^2 W_r}{\partial r_{A,i} \partial r_{B,j}}\right) = \left(\frac{d\mathbf{r}_B}{d\mathbf{p}_{Ar}}\right)^{-1}, \quad (25)$$

we have

$$K(\mathbf{r}_A, \mathbf{r}_B, t) = \frac{1}{(2\pi i\hbar)^{N/2}} \sum_r |D_r|^{1/2} \exp\left[i(W_r/\hbar - \alpha_r \pi/2)\right]. \quad (26)$$

Integrable systems can be described by action angle variables $(\mathbf{I}, \boldsymbol{\theta})$, where $\boldsymbol{\theta} = (\theta_1, \theta_2, \ldots)$. The dynamics of the system is then restricted to a torus in phase space. The action variables are constants of the motion, whereas the angular velocities follow immediately from Hamilton's equations of motion,

$$\frac{d\boldsymbol{\theta}}{dt} = \nabla_{\mathbf{I}} H(\mathbf{I}) = \boldsymbol{\omega}(\mathbf{I}), \quad \boldsymbol{\omega} = (\omega_1, \ldots, \omega_N). \quad (27)$$

The action along a path is determined by the initial and final angles $\boldsymbol{\theta}_A, \boldsymbol{\theta}_B$. We then have

$$W_r(\mathbf{r}_A, \mathbf{r}_B, t) = \mathbf{I}_r \cdot (\boldsymbol{\theta}_B - \boldsymbol{\theta}_A) - H(\mathbf{I}_r)t. \quad (28)$$

By means of the relation $(\boldsymbol{\theta}_B - \boldsymbol{\theta}_A) = \boldsymbol{\omega}(\mathbf{I}_r)t$ one can rewrite D_r as

$$D_r(\boldsymbol{\theta}_A, \boldsymbol{\theta}_B, t) = \left(\frac{d\boldsymbol{\theta}_A}{d\mathbf{I}_r}\right)^{-1} = \frac{1}{t^N \det(\partial\omega_i/\partial I_{rj})}. \quad (29)$$

To obtain the density of energy eigenvalues $\rho(E)$ the propagator $K(\mathbf{r}_A, \mathbf{r}_B, t)$ has to be Fourier transformed with respect to time. If we now take the trace we have to sum over all configurations that return to the initial point $\mathbf{r}$ after a time t. As a torus is periodic in θ_i with period 2π, taking the trace requires a summation over all paths connecting the points

$$\theta_{B_i} = \theta_{A_i} + k_i 2\pi, \quad k_i \in \mathbb{N}. \quad (30)$$

As the generalized momenta remain constant throughout the process, we can write

$$\int d^N \mathbf{r} K(\mathbf{r}, \mathbf{r}, t) = \sum_{\mathbf{M}} \int_0^{2\pi} d^N \boldsymbol{\theta} K(\boldsymbol{\theta} + 2\pi\mathbf{M}, \boldsymbol{\theta}, t). \quad (31)$$

The vector $\mathbf{M}$ of dimension N with integer entries determines the topology of the periodic orbits. The contribu-

tion for $\mathbf{M}=\mathbf{0}$ is the so-called Thomas-Fermi term

$$\rho_{TF}(E)=\frac{1}{2\pi\hbar^N}\int\int d\mathbf{p}\,d\mathbf{r}\,\delta[E-H(\mathbf{r},\mathbf{p})]. \tag{32}$$

With $\mathbf{I}_\mathbf{M}$ the vector of actions along the different directions of the torus we have in the semiclassical approximation

$$\rho(E)=\rho_{TF}(E)+\frac{(2\pi)^N}{\pi\hbar}\mathrm{Re}\,\frac{1}{(2\pi i\hbar)^{N/2}}\sum_{\mathbf{M}}\int_0^\infty dt\frac{\exp\{[i(2\pi\mathbf{I}_\mathbf{M}\mathbf{M}-H(\mathbf{I}_\mathbf{M})t+Et)/\hbar]-i\boldsymbol{\alpha}_\mathbf{M}\cdot\mathbf{M}\pi/2\}}{t^{N/2}|\det(\partial\omega_i/\partial\mathbf{I}_{\mathbf{M}_j})|^{1/2}}. \tag{33}$$

This integral must be evaluated in stationary phase. The first derivative of the argument of the exponential is

$$\begin{aligned}\hbar\frac{d}{dt}(\text{phase})&=(2\pi\mathbf{M}-t\nabla_\mathbf{I}H)\cdot\frac{\partial\mathbf{I}_\mathbf{M}}{\partial t}-H(\mathbf{I}_\mathbf{M})+E\\&=E-H(\mathbf{I}_\mathbf{M}(t_\mathbf{M}(E))).\end{aligned} \tag{34}$$

The requirement that the phase be stationary fixes the time to be $t_\mathbf{M}(E)$, the time of revolution around an orbit of topology $\mathbf{M}$ at energy E. The second derivative of the phase with respect to time is

$$\frac{1}{\hbar}\frac{d}{dt}[E-H(\mathbf{I}_\mathbf{M})]=-\boldsymbol{\omega}(\mathbf{I}_\mathbf{M})\cdot\frac{\partial\mathbf{I}_\mathbf{M}}{\partial t}, \tag{35}$$

where the last equality holds because of

$$\boldsymbol{\omega}[\mathbf{I}_\mathbf{M}(t)]t=2\pi\mathbf{M}. \tag{36}$$

With the definition

$$A_\mathbf{M}^2(E)=\frac{(2\pi)^{N-1}}{(i\hbar)^{N+1}(t_\mathbf{M})^N|\det(\partial\omega_i/\partial\mathbf{I}_{\mathbf{M}_j})|[\vec{\omega}(\mathbf{I}_\mathbf{M})\cdot\partial\mathbf{I}_\mathbf{M}(t_\mathbf{M})/\partial t]}, \tag{37}$$

the final result for the density of eigenvalues reads [8]

$$\rho(E)=\rho_{TF}(E)+2\mathrm{Re}\sum_{\mathbf{M}}A_\mathbf{M}(E)\exp\{i[2\pi\mathbf{M}\cdot(\mathbf{I}_\mathbf{M}/\hbar-\vec{\alpha}_\mathbf{M}/4)]\}. \tag{38}$$

We need to evalute these amplitudes for a 2D square billiard with sidelength $L_x=L_y=\pi$, for which the classical Hamiltonian in action-angle variables $(\boldsymbol{\theta},\mathbf{I})$ is obtained from the association $\mathbf{I}=(\hbar k_xL_x/\pi,\hbar k_yL_y/\pi)$, and $E=\hbar^2\mathbf{k}^2$, so that

$$H(I_x,I_y)=I_x^2+I_y^2. \tag{39}$$

Then the angular velocity becomes

$$\boldsymbol{\omega}=2\mathbf{I}, \tag{40}$$

and the actions

$$\mathbf{I}_\mathbf{M}=\pi\mathbf{M}/t. \tag{41}$$

For the square one has non-negative actions I_x, I_y and, by Eq. (38), contributions for positive times only. Thus the admissible values of $\mathbf{M}$ that contribute are non-negative integers. With the time

$$t_\mathbf{M}(E)=\pi|\mathbf{M}|/\sqrt{E}, \tag{42}$$

one calculates the amplitudes (37)

$$A_\mathbf{M}(E)=\frac{e^{-i\pi/4}}{\hbar^{3/2}E^{1/4}\sqrt{|\mathbf{M}|}}. \tag{43}$$

To obtain the amplitudes A_p for the density of states in k, Eq. (9), one uses $\rho(k)=\rho(E)dE/dk$ and takes into account that the lengths of orbits p with topology $\mathbf{M}$,

$$L_p=2\pi|\mathbf{M}|, \tag{44}$$

coincide for $\mathbf{M}=(M_x,M_y)$ and (M_y,M_x). One thus finds

TABLE I. Observed and calculated differences in amplitude for some orbits in the 2D square. The first column gives the length, the second the topological numbers $\mathbf{M}=(M_x,M_y)$, the third and fourth the amplitudes $A_{BT}/2$ and A_S calculated from Eq. (60), and the last two the observed values. To measure A_S, the difference between the Dirichlet and Neumann bc density of states has been Fourier transformed with $D=1$ in Eq. (11).

L_p	(M_x,M_y)	$A_{BT,t}/2$	$A_{S,t}$	A_{obs}	$A_{S,obs}$
6.28	(0,1); (1,0)	0.500	1	0.494	0.974
8.88	(1,1)	0.420	0	0.411	0
12.56	(0,2); (2,0)	0.354	1	0.345	0.974
14.05	(1,2); (2,1)	0.669	0	0.668	0
17.77	(2,2)	0.297	0	0.296	0

$$A_p = \begin{cases} \frac{\exp[-i\pi/4]}{2\sqrt{|\mathbf{M}|}} & \text{for } M_x = M_y \\ \frac{\exp[-i\pi/4]}{\sqrt{|\mathbf{M}|}} & \text{for } M_x \neq M_y \end{cases} . \quad (45)$$

Fourier transforms confirm these amplitudes except for topologies with $M_x = 0$ or $M_y = 0$ (see Table I). These are affected by symmetrization, as discussed next.

C. Symmetry decomposition of the propagator

As mentioned before, the wave function in the unfolded square is symmetric about the symmetry axis for Neumann boundary conditions and antisymmetric for Dirichlet boundary conditions. The propagator for these functions can be split into a symmetric and an antisymmetric part. The symmetry operation considered now is the reflection at the middle of the unfolded square (see Fig. 7). This symmetry introduces new equivalent points and further contributions to the trace equation (31) than just those indicated by Eq. (30). For the following analysis, we will only consider one of the boundaries, say BC, so that the results have to be multiplied by 2 to account for the second boundary orbit AD.

We will analyze the symmetry decomposition for the reflection described by

$$g[(x,y)] = (-x,y) . \quad (46)$$

There is an additional reflection on the x axis that can be dealt with similarly. We will proceed with just this symmetry and then extend to the full desymmetrization later. And since the y-coordinate plays a minor role for the above reflection, we will suppress it in the expressions for the propagator that follow. The projection operators onto even and odd subspaces are

$$P_+ \equiv \frac{1}{2}(e+g),$$
$$P_- \equiv \frac{1}{2}(e-g). \quad (47)$$

The propagator can now be decomposed

$$K = K_+ + K_- \quad (48)$$

with

$$K_+ \equiv P_+ K P_+ \quad , \quad K_- \equiv P_- K P_- . \quad (49)$$

More precisely, we have

$$\begin{aligned} P_+ K P_+ &= \frac{1}{4}(e+g)K(e+g) \\ &= \frac{1}{4}(eKe + gKe + eKg + gKg) \\ &= \frac{1}{4}[K(x,x',t) + K(-x,x',t) \\ &\quad + K(x,-x',t) + K(-x,-x',t)] . \end{aligned} \quad (50)$$

As announced before, the y coordinates are suppressed in the propagators. For motion on a torus the coordinates x and x' can be replaced by the angles θ_x and θ'_x. For the trace we can identify $x = x'$ and $\theta_x = \theta'_x$ and use

$$\begin{aligned} K(x,x,t) &= K(-x,-x,t), \\ K(-x,x,t) &= K(x,-x,t) \end{aligned} \quad (51)$$

to arrive at

$$P_+ K P_+ = \frac{1}{2}[K(\theta_x,\theta_x,t) + K(\theta_x,-\theta_x,t)] . \quad (52)$$

Similar arguments result in the expression

$$P_- K P_- = \frac{1}{2}[K(\theta_x,\theta_x,t) - K(\theta_x,-\theta_x,t)] \quad (53)$$

for K_-.

As above, taking the trace corresponds to an integration over all θ_x and θ_y and a summation over different topologies $\mathbf{M}$. This time, however, we have to allow for all values of M_x, M_y since we start from the propagator on the torus with periodic boundary conditions. Then $\mathbf{M}$ with negative components correspond to different orbits that are not on tori with positive components. All of these orbits contribute to the same length L_p and thus affect the multiplicity of the amplitude. Hence,

$$\begin{aligned} \operatorname{tr} K|_{b.o.} = \frac{1}{2}\sum_{\mathbf{M}} \int_{-\pi}^{\pi} d\theta_x d\theta_y [K(\theta_x, \theta_x + 2\pi M_x, t) \\ + K(\theta_x, -\theta_x + 2\pi M_x, t)] \end{aligned} \quad (54)$$

for symmetric and

$$\begin{aligned} \operatorname{tr} K|_{b.o.} = \frac{1}{2}\sum_{\mathbf{M}} \int_{-\pi}^{\pi} d\theta_x d\theta_y [K(\theta_x, \theta_x + 2\pi M_x, t) \\ - K(\theta_x, -\theta_x + 2\pi M_x, t)] \end{aligned} \quad (55)$$

for antisymmetric states.

An evaluation of the second term yields a factor of 2π from the integration over the θ_y component, since the integrand does not depend explicitly on θ_y. The propagator

$$K(\theta_x, -\theta_x, t)$$

$$= \frac{1}{(2\pi i\hbar)} \sum_r |D_r|^{1/2} \exp\left[i\left(\frac{W_r}{\hbar} - \alpha_r \pi/4\right)\right] \quad (56)$$

does depend on the second variable θ_x through the action [compare (28) and Fig. 7]

$$W_r = \left(\theta_x^2 + \pi^2 M_y^2\right)/t . \quad (57)$$

When evaluated in stationary phase, one finds

$$\int_{-\pi}^{\pi} d\theta_x d\theta_y K[(\theta_x, \theta_y + 2\pi M_y), (-\theta_x, \theta_y), t]$$

$$\cdots \left(\frac{\pi}{4i\hbar}\right)^{1/2} \frac{1}{\sqrt{t}} \sum_{M_y} e^{i\pi^2 M_y^2/t\hbar} . \quad (58)$$

This is the contribution of the boundary orbit, the orbit that lies on the symmetry axis of the system. As the

opposite side of the square is a symmetry axis as well, there are two boundary orbits contributing. Thus the correction has to be multiplied by 2.

The same procedure now has to be repeated for the reflection on the y axis. The final result is that the symmetry decomposition (55) picks up a factor 1/4 and a total of four contributions from paths connecting (θ_x, θ_y) to $(\pm\theta_x, \pm\theta_y)$. If $\mathbf{M} = (M_x, M_y)$ denotes the topologies of paths, then one has to consider three cases:

(i) If $M_x \neq 0$ and $M_y \neq 0$ and $M_x \neq M_y$, then there are eight paths of different topologies on the torus contributing to the same length L_p, namely, $\mathbf{M} = (\pm M_x, \pm M_y)$ and $(\pm M_y, \pm M_x)$. Together with the 1/4 from the desymmetrization, one recovers the Berry-Tabor amplitude (45).

(ii) If $M_x \neq 0$ and $M_y \neq 0$ and $M_x = M_y$, then there are just four paths of different topology on the torus, and one again recovers the Berry-Tabor amplitude (45).

(iii) If $M_x = 0$ or $M_y = 0$, then first of all one has only four different paths and thus in leading order an amplitude that is half that of Berry and Tabor. Second, there are contributions from the reflected paths, as described by (58). Combining both cases $M_y \neq 0$ and $M_x \neq 0$, one finds for the amplitude contributing to the length $L_p = 2\pi M_y$ in the symmetric (subscript +) and antisymmetric subspaces (subscript −) the form

$$A_\pm = \frac{e^{-i\pi/4}}{\sqrt{M_y}} \pm k^{-1/2} \tag{59}$$

$$A_\pm = \frac{1}{2} A_{BT} \pm A_S k^{-1/2}, \tag{60}$$

respectively. A_{BT} is the amplitude assigned to the orbit by the theory of Berry and Tabor [8], as given in Eq. (45).

The term A_{BT} can be determined as the average of the amplitudes in Fourier transforms of the spectra for Dirichlet and Neumann boundary conditions. The subdominant symmetry correction A_S can be determined from a Fourier transform of the difference in the spectra with Neumann and Dirichlet boundary conditions, weighted with $D = 1$ in the equivalent of Eq. (11). As shown in Table I, these amplitudes are in agreement with the observations that the correction A_S is independent of M_y, the number of traversals of the orbit. Thus the decrease or increase in amplitude in Fig. 3, too, does not depend on the number of traversals.

D. The case of the triangle

The analysis of the triangle eigenvalues proceeds in a similar fashion with the additional difficulty that the symmetry group is larger (three reflections and three rotations) and gives rise not only to one-dimensional representations but also to two-dimensional ones (as discussed, e.g., in [14]). Continuing the unfolding of Fig. 4 one finds that twelve copies of the triangle fit into a rectangle of side length $3L$ by $\sqrt{3}L$, which then covers the plane by translations. The symmetry reduced Greens functions can be obtained by a summation over all symmetry images and their translations. The orbit shown in Fig. 4 is invariant under a reflection of the original triangle, translated by half the side length of the rectangle along both sides. It contributes in several of the symmetry subspaces. When summed over all symmetry classes of the triangle for the case of Dirichlet boundary conditions on the outer boundary, one set of contributions survives. In the case of Neumann boundary conditions, all contributions cancel. This is in agreement with the numerical observations.

An alternative approach to the periodic orbit contributions is based on an application of the Poisson summation formula to the density of states. For this it is useful to unscramble the restrictions on the quantum numbers. For $m > 0$, one can take all $n > m$ (doubly degenerate) and $n = m$ (nondegenerate), with eigenvalues

$$E_{n,m} = \frac{4\pi^2}{3h^2}(n^2 + m^2 + nm).$$

For $m < 0$, the restriction $l = -m - n$ and $l \leq m$ can be resolved by putting $n = -2m + j$ and $l = m - j$ with $m = -1, -2, \ldots$ and $j = 0$ (nondegenerate) and $j = 1, 2, \ldots$ (doubly degenerate). The eigenvalues become

$$E_{m,j} = \frac{4\pi^2}{3h^2}(3m^2 + j^2 - 3mj).$$

For the restrictions on the summation we need the Heaviside step function

$$\Theta(x) = \begin{cases} 0 & x < 0 \\ 1/2 & x = 0 \\ 1 & x > 0 \end{cases}. \tag{61}$$

In the Dirichlet case, the density of states becomes

$$\begin{aligned}\rho_D(E) = &\sum_{n,m} \Theta(n)\Theta(m)\delta\left(E - \frac{4\pi^2}{3h^2}(n^2 + m^2 + nm)\right) \\ &+2\sum_m \Theta(-m)\Theta(j)\delta \\ &\times\left(E - \frac{4\pi^2}{3h^2}(3m^2 + j^2 - 3mj)\right) \\ &-2\sum_m \Theta(m)\delta\left(E - \frac{4\pi^2}{3h^2}m^2\right) + 1/4\delta(E).\end{aligned}$$

For Neumann boundary conditions, the states with $m = 0$ have to be added: $l = n = 0$ is nondegenerate, the others with $n = -l = 1, 2, \ldots$ are doubly degenerate. Thus the density of states for Neumann boundary conditions becomes

$$\begin{aligned}\rho_N(E) = &\rho_D(E) \\ &+2\sum_n \Theta(n)\delta\left(E - \frac{4\pi^2}{3h^2}n^2\right).\end{aligned}$$

The Poisson summation formula applied to the difference in eigenvalue density for the two boundary conditions gives

$$\sum_n \Theta(n)\delta\left(E - \frac{4\pi^2}{3h^2}n^2\right) = \sum_m \frac{\sqrt{3}h}{4\pi\sqrt{E}} e^{-imh\sqrt{3E}}.$$

In a Fourier transform in $k = \sqrt{E}$, this gives rise to a sequence of peaks at a spacing of $\Delta l = \sqrt{3}h = 3L/2$. This is the length of the triangle orbit shown in Fig. 4. The terms in the double sum give rise to contributions with weight $1/E = 1/k^2$. Thus, there are corrections related to this orbit in Dirichlet boundary conditions, but not in Neumann boundary conditions as observed.

IV. CONCLUDING REMARKS

We have examined some of the consequences of the semiclassical Balian and Duplantier theory [5] for electromagnetic eigenvalue problems in integrable domains and have studied the connection to Berry and Tabor's theory [8] for the appropriate boundary conditions. Some examples of perfect and less perfect cancellations of orbits with an odd number of reflections were identified and explained within the Berry and Tabor theory [8] and symmetry extensions thereof.

The calculations also highlight the fact that, at least in the separable systems, the cancellations of some orbits are due to the superposition of both the TE and TM modes. If the detecting system interacts with certain electric or magnetic field components only, all orbits can appear in the Fourier transform of the signal. Actually, if detector and source are sufficiently localized, all returning orbits (even nonperiodic ones), should contribute.

What cannot be tested using separable cylindrical resonators is the amplitude modification due to the rotation of polarizations. To this end one has to rely on resonators like the 3D Sinai billiard and variants thereof. However, since the density of orbits increases so rapidly and since the short orbits rather often are planar without phase rotations, this modification of amplitudes can only be detected in high resolution Fourier transforms, requiring very long eigenvalue sequences. The present calculations suggest certain geometries in which the proliferation effect of periodic orbits can be reduced, thus easing the task of identifying orbits with a modified amplitude: in perturbations of circular cavities, orbits with an odd number of reflections are partly suppressed, and in perturbations of spherical cavities, they will presumably not contribute at all, thus reducing the number of lines in the Fourier transforms. And if the perturbation is suitably chosen, the whispering gallery modes can disappear. One should be careful, however, not to introduce new symmetries that will bring some of these suppressed orbits back up in amplitude.

ACKNOWLEDGMENT

We thank E.B. Bogomolny for pointing out the work of Balian and Duplantier.

[1] H.-J. Stöckmann and J. Stein, Phys. Rev. Lett. **64**, 2215 (1990); J. Stein and H.-J. Stöckmann, *ibid.* **68**, 2867 (1992).
[2] S. Sridhar, Phys. Rev. Lett. **67**, 785 (1991)
[3] H.-D. Gräf, H. L. Harney, H. Lengeler, C. H. Lewenkopf, C. Rangacharyulu, A. Richter, P. Schardt, and H. A. Weidenmüller, Phys. Rev. Lett. **69**, 1296 (1992).
[4] B. Eckhardt, in *Quantum Chaos*, edited by G. Casati, I. Guarneri, and U. Smilansky (North-Holland, Amsterdam, 1993), p. 77.
[5] R. Balian and B. Duplantier, Ann. Phys. (N.Y.) **104**, 300 (1977).
[6] J. D. Jackson, *Classical Electrodynamics* (John Wiley & Sons, New York, 1975).
[7] S. Flügge, *Handbuch der Physik, Band XVI, Elektromagnetische Felder und Wellen* (Springer-Verlag, Berlin, 1958).
[8] M. V. Berry and M. Tabor, Proc. R. Soc. London Ser. **A 349**, 101 (1976); J. Phys. A **10**, 371 (1977).
[9] R. Balian and C. Bloch, Ann. Phys. (N.Y.) **60**, 401 (1970); **69**, 76 (1972).
[10] J. M. Robbins, Phys. Rev. A **40**, 2128 (1989); B. Lauritzen, *ibid.* **43**, 603 (1991); P. Cvitanović and B. Eckhardt, Nonlinearity **6**, 277 (1993).
[11] B. Eckhardt, Acta Phys. Pol. **24**, 773 (1993).
[12] A. Hobson, J. Math. Phys. **16**, 2210 (1975).
[13] M. V. Berry and K. E. Mount, Rep. Prog. Phys. **35**, 315 (1972).
[14] C. Jung, Can. J. Phys. **58**, 719 (1980).